

Formation of Flat, Homogeneous Surfaces of Organized Molecular Films of Three-Armed Polymerizable Amphiphiles with Metal-Scavenging Properties

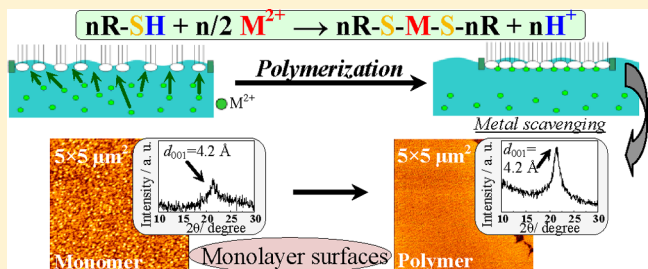
Atsuhiro Fujimori,^{*†} Makoto Taguchi,[‡] Sho Hakozaki,[§] Kenji Kamishima,[†] and Bungo Ochiai[§]

[†]Graduate School of Science and Engineering, and [‡]Department of Functional Material Science, Faculty of Engineering, Saitama University, 255 Shimo-okubo, Sakura-ku, Saitama 338-8570, Japan

[§]Graduate School of Science and Engineering, Yamagata University, Yonazawa, Yamagata 992-8510, Japan

S Supporting Information

ABSTRACT: Surface complexing (i.e., metal-bridged polymerization in this study) of a three-armed amphiphilic compound with metal-scavenging properties has been investigated using the surface pressure–area (π -A) isotherms of a Langmuir monolayer from the subphase. Inductively coupled plasma mass spectrometry (ICP-MS) was also carried out on eluted solutions from corresponding multilayers of the solid. Furthermore, the molecular arrangement and surface morphology of organized molecular films of the resultant comb polymer were estimated by in-plane and out-of-plane X-ray diffraction (XRD) and by atomic force microscopy. From an analysis of the wide-angle X-ray diffraction of the corresponding monomer in the bulk, the long hydrocarbon chains are observed to pack hexagonally in the solid state. Compared to their monolayer on distilled water as the subphase, a polymerized monolayer on a buffer solution containing Cd^{2+} ions is remarkably expanded at 15 °C. From ICP-MS and IR measurements, it is found that this monolayer stoichiometrically contains Cd^{2+} ions on the –SH group. It is found by XRD that highly ordered layer structures and regular 2D lattices are constructed in the organized molecular films of the Cd-bridged comb polymer. Furthermore, the surface morphology of Langmuir–Blodgett films fabricated from the monolayers on a buffer solution containing Cd^{2+} and Pd^{2+} shows flat and smooth domains upon metal scavenging and polymerization.



INTRODUCTION

Organized molecular films¹ can be developed as candidates for biomimetic models² and molecular electronic devices,^{3,4} which are of considerable interest in the fundamental sciences because of their potential applications.⁵ In addition to lipids and proteins interacting with hydrocarbons, various amphiphiles with functional groups, including π - and d-electron systems, or polymerizable groups have been synthesized to obtain monolayer assemblies with well-defined molecular arrangements.⁶

Metal ions play an important role in the organization of biological and supramolecular systems.^{7,8} A typical example of this role is illustrated by the effect of metal ions on the properties of Langmuir and Langmuir–Blodgett (LB) films.⁴ The observation of such an effect can be dated to the pioneering work of Blodgett in 1935, where metal ions were found to be effective in fabricating well-defined LB films.⁹ Currently, metal ions are widely used to modulate the surface properties of interfacial films. Generally, two employments of metal ions can be considered. The first is to utilize metal ions to stabilize the monolayers and fabricate well-defined LB films. The second is to utilize metal ions to functionalize interfacial films. For the latter case, a series of functional organic ligands

have been designed, and their metal-ion-regulated properties were investigated.^{10–15}

In recent years, the potential exhaustion of and increasing demand for rare metal and rare earth elements have become objects of public concern worldwide. The effective scavenging of rare metals or rare earth elements is therefore an important subject for the present industry. Useful rare metals such as uranium and vanadium are dissolved at ultratrace levels in the Pacific Ocean. These metals are carried on the ocean current, passing over to the continent of Asia. If it is possible to scavenge these useful rare metals, then they can be effectively utilized, and the present practice of importing them from a limited number of countries can be stopped. Thus a stable, long-term supply of resources can be ensured. Figure 1 shows the metal-scavenging polymerization reaction carried out by a polymerizable trithiol derivative from a solution containing Cu^{2+} ions. A uniformly blue Cu^{2+} solution becomes transparent upon precipitation of the metal-bridged polymer. Previously, the ability of this polymerizable trithiol derivative to scavenge

Received: March 16, 2012

Revised: June 26, 2012

Published: June 26, 2012



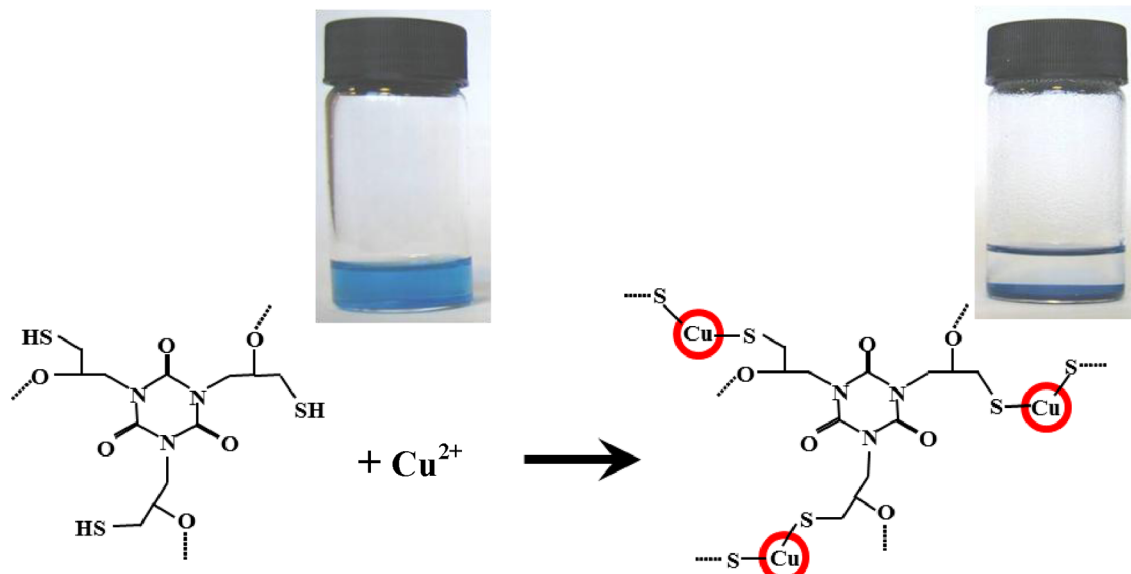
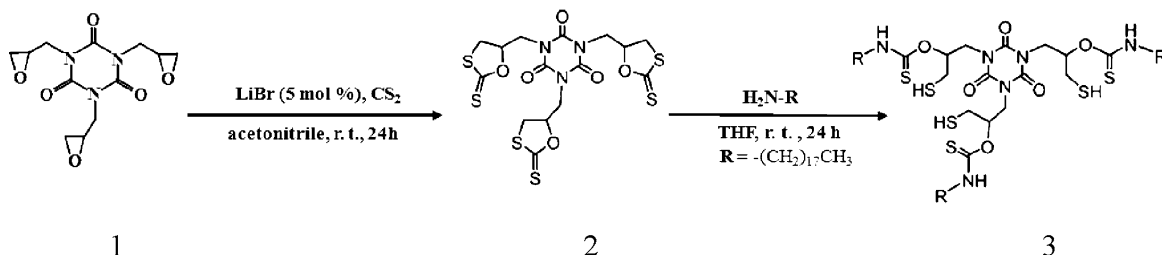


Figure 1. Bivalent metal (Cu^{2+}) scavenging reaction of a trithiol derivative.

Scheme 1. Synthesis Scheme of 3C18-PMTT from Trifunctional Epoxide



Pd^{2+} has been reported.^{16,17} Although the scavenging of bivalent ions is shown in these cases, this compound can be widely applied to other metal valences or to any noble metal.^{18,19} Essentially, sulfur-containing polymers are applied as optic,^{20,21} metal-scavenging,^{22,23} and adhesive^{24,25} materials owing to their high atomic refractivity, metal complexing ability, and high reactivity. Furthermore, by using the Langmuir technique and by taking advantage of the amphiphilic ability of this type of material, it may be possible to scavenge several metal ions, including rare metal and rare earth elements, from the subphase. Simultaneously, metal-scavenged polymer is formed at the air/water interface and the scavenged metals in the films are arranged in the same plane. In addition, by using the Langmuir–Blodgett (LB) technique, it is possible to introduce metal ions in a highly ordered layer structure on the nanometer scale. In this case, the scavenged metals may be regularly arranged in repeating units in the *ab* plane, situated between the insulated organic parts aligned along the *c* axis. This type of multilayered construct acts in a similar way to a nanometer-sized capacitor. In other words, it is expected that a practical use of amphiphilic metal-scavenged polymer will be as a connector to produce new nanomaterials, such as nano-electronic devices.

In the present study, a new three-armed amphiphilic compound with metal-scavenging properties, 1,3,5-tris[2-N-octadecylamidothiocarboxy-3-propanemercapto]-1,3,5-triazine-2,4,6-trion,^{16,17} (from here on abbreviated as 3C18-PMTT, see Scheme 1), was synthesized as a metal-scavenging monomer. The solid-state structure, monolayer behavior, molecular

arrangement, and surface morphology of organized molecular films of this monomer and corresponding polymers were investigated via wide-angle X-ray diffraction (WAXD), small-angle X-ray scattering (SAXS), surface pressure–area (π – A) isotherms, infrared (IR) spectroscopy, in-plane and out-of-plane X-ray diffraction (XRD), and atomic force microscopy (AFM) measurements. Furthermore, using a Langmuir film on a buffer solution containing Cd^{2+} and Pd^{2+} ions, the surface-complexing behavior of this amphiphile with metal-scavenging properties has been monitored and estimated via a π – A isotherm. Inductively coupled plasma mass spectrometry (ICP-MS) has also been used on corresponding multilayers arising from eluted solutions from the solid substrate.

EXPERIMENTAL SECTION

Synthesis of 3C18-PMTT. Carbon disulfide (3.60 mL, 59.8 mmol; Kanto Chemical) was added dropwise to a solution of trifunctional epoxide 1 (2.97 g, 10.0 mmol) and LiBr (0.043 g, 0.500 mmol) in acetonitrile (10.0 mL; Kanto Chemical) at room temperature. The solution was stirred at room temperature for 24 h. The resulting suspension was filtered, and the residual solid was washed with chloroform (200 mL; Kanto Chemical). The obtained yellow powder was dried in *vacuo* to give 3 (4.42 g, 84%). This was then reacted with octadecylamine to obtain the corresponding 3C18-PMTT (Scheme 1).^{18,19} The detailed synthesis procedure and characterization of chemical structure by NMR, IR, and elemental analysis and yield of the synthesized compound have already been described in refs 18 and 19. The design concept for choosing the star-shaped structure of 3C18-PMTT is a high coverage of the water surface on the subphase, including metal ions by the large size of the backbone as hydrophilic groups. Three octadecyl hydrophobic chains are introduced into this

compound in order to obtain the overall amphiphilicity of the molecules. It is expected that a high metal-scavenged ratio of this amphiphile as a monolayer on the water surface is achieved. In addition, there is the anticipation of the formation of a low defect surface induced by surface-complexing macromolecules.

Structural Estimation in the Bulk. The packing modes of 3C18-PMTT in the crystalline phase were examined using a WAXD instrument (Rigaku, R-axis Rapid, Cu K α radiation, 40 kV, 200 mA) equipped with a graphite monochromator. The layer structures of the comb copolymers were characterized using a SAXS instrument (Rigaku, NANO-Viewer, Cu K α radiation, 40 kV, 30 mA). Thermal analyses were carried out by using a Seiko Instruments model DSC200 differential scanning calorimeter (DSC). The DSC measurements were performed at a standard scanning rate of 10.0 °C min $^{-1}$. A sample mass of ca. 5.00 mg was used for all DSC measurements. As usual, the scanning of DSC measurements and the heating and cooling cycle were repeated twice in order to examine the difference between the peak position and transition enthalpy in the first and second heatings.

Formation of Monolayers on the Water Surface and Observation of the Molecular Arrangement in the Films. Monolayers of 3C18-PMTT were formed by spreading a chloroform solution (ca. 1.0×10^{-4} M) onto a distilled water (18.2 MΩ cm) surface or buffer solution containing Cd $^{2+}$ and Pd $^{2+}$ ions. Subphase conditions of the Cd $^{2+}$ buffer solution containing Cd $^{2+}$ and Pd $^{2+}$ ions corresponding to 3.8×10^{-4} mol/L CdCl₂, 5.0×10^{-5} mol/L KHCO₃ (pH 6.21), 1.5×10^{-4} mol/L PdCl₂, and 5.0×10^{-5} mol/L KHCO₃ (pH 6.21). Pd is a representative rare metal element commonly used as a catalyst, inlay, or within electrical devices. After 5 min of chloroform evaporation, the surface pressure-area (π -A) isotherms were recorded at a compression speed of 0.08 mm s $^{-1}$. The air/water interface was kept at a constant temperature of 15 °C by circulating thermostatted water around the trough. Measurements of the monolayer properties and LB film transfer were carried out using a USI-3-22 Teflon-coated LB trough (USI Instruments). The hydrophobic side chains on the outermost surface of the Z-type²⁶ LB films that had been transferred onto solid substrates were exposed to air.

Molecular Arrangement in the Films. The surface morphologies of the transferred films were observed using a scanning probe microscope (atomic force microscopy, Seiko Instrument, SPA300 with SPI-3800 probe station) and microfabricated rectangular Si cantilevers with integrated pyramidal tips by applying a constant force of 1.4 N m $^{-1}$. In this study, AFM observation is performed in tapping mode. XRD samples were transferred onto glass substrates by the Langmuir–Blodgett method (20 layers, subphase temperature 15 °C, and transfer surface pressure of 15 mN m $^{-1}$). The large spacing between the layer structures of the films transferred onto the glass substrates was measured using an out-of-plane X-ray diffractometer (Rigaku, Rint2200 V, Cu K α radiation, 40 kV, 100 mA) equipped with a graphite monochromator. The in-plane spacing of the 2D lattice of the films was determined using an X-ray diffractometer with different geometrical arrangements^{27,28} (Bruker AXS, MXP-BX, Cu K α radiation, 40 kV, 40 mA, an instrument specially made to order) and equipped with a parabolic graded multilayer mirror. The X-rays were incident at an angle of 0.2°, and the films were slowly scanned at a speed of 0.05°/80 s. Thus, in-plane XRD measurements were carried out at monomolecular resolution.

RESULTS AND DISCUSSION

Estimation of Fine Structure for 3C18-PMTT in the Bulk. Figure 2 shows WAXD and SAXS patterns and profiles of the obtained 3C18-PMTT. The profile of the 3C18-PMTT monomer indicates that it possesses long alkyl chains through the sharp peaks observed at $2\theta = 2.7$, 5.1, and 21.3° ($d_{100} = 33.5$, 17.5, and 4.2 Å, respectively). From this, the polycrystalline structure of 3C18-PMTT is determined to correspond to the formation of a hexagonal subcell by long alkyl chains in the *ab* plane. This structure is similar to that observed in

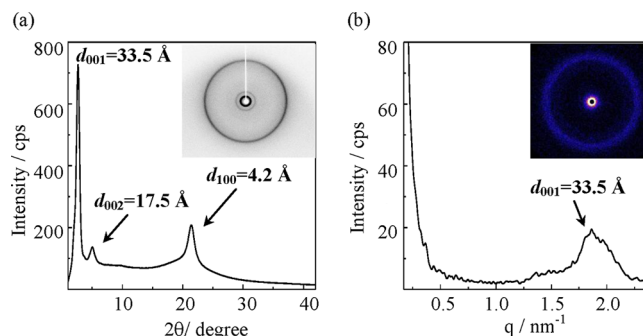


Figure 2. (a) WAXD and (b) SAXS patterns and profiles of 3C18-PMTT in the bulk.

conventional side-chain crystalline comb polymers.^{29,30} The WAXD profile of 3C18-PMTT shows a long spacing of 33.5 Å along the *c* axis, but this is much smaller than the calculated value for a double-layered structure with head-to-head and tail-to-tail orientations. From the SAXS measurements, no spacing longer than 33.5 Å was detected. Therefore, spacings of 33.5 and 17.5 Å were assigned to (001) and (002) reflections, respectively. The existence of a second-order reflection implies the formation of a highly ordered layer structure for this material.

Figure 3 and Table 1 show the DSC thermogram and calculated thermodynamic parameters of 3C18-PMTT in the

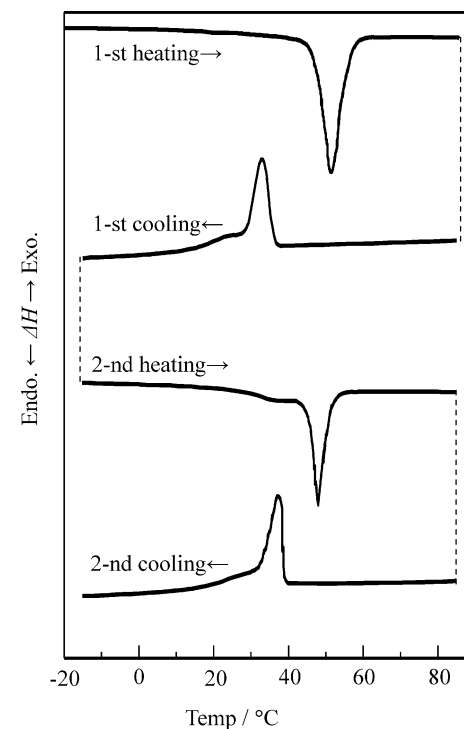


Figure 3. DSC thermograms of 3C18-PMTT (scanning rate, 10 °C min $^{-1}$).

bulk, respectively. The appearance of relatively sharper melting peaks on the lower-temperature side highlights the formation of a typical polycrystalline structure that is observed for general long-chain compounds.^{31,32} Hence, models of chain packing and the orientation of 3C18-PMTT can be drawn as those in Figure 4. In accordance with the SAXS result, a remarkable tilted orientation (56° with respect to the surface normal) for

Table 1. Thermodynamic Parameters of 3C18-PMTT Estimated from a DSC Thermogram

first heating	
T_m (°C)	ΔH (kcal/mol)
51.7	
T_c (°C)	ΔH (kcal/mol)
32.3	
second heating	
T_m (°C)	ΔH (kcal/mol)
46.3	16.2
second cooling	
T_c (°C)	ΔH (kcal/mol)
36.6	-13.6

3C18-PMTT is proposed. The formation of a subcell structure packed with long-chain hydrocarbons is supported by the existence of the d_{001} reflection and by the sharper melting peaks.

Monolayer Behavior and Surface Morphology of 3C18-PMTT. Figure 5 shows the π -A isotherms of 3C18-PMTT on distilled water and the buffer solution containing Cd²⁺ ions at 15 °C. The estimated collapse surface pressure and limiting area are also shown. 3C18-PMTT forms a stable condensed monolayer in a single condensed state. When metal ions were present in the subphase, significant changes were observed. For example, for the subphase containing Cd²⁺ ions, the monolayer exhibited a relatively low collapse surface pressure (51.1–32.5 mN m⁻¹) and the π -A isotherms were only slightly expanded (118.6–136.8 Å/monomer unit). It seems that these changes occurred by cadmium ions being scavenged (that is to say, Cd-bridged polymerization) from the buffer solution containing Cd²⁺ ions. Figure S1 in the

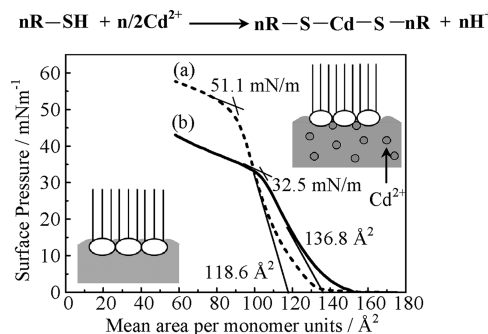


Figure 5. Surface pressure-area isotherms of monolayers (a) on the distilled water surface and (b) on the surface of a buffer solution containing Cd²⁺ in 3C18-PMTT at 15 °C.

Supporting Information shows the IR spectra of 3C18-PMTT in the bulk, LB multilayers of 3C18-PMTT, and LB multilayers of poly[(3C18-PMTT)₂Cd] on a CaF₂ substrate. In these spectra, the position of metal scavenging in the 3C18-PMTT molecules corresponds to the mercapto group. The S-H stretching vibrational band appears at around 2560 cm⁻¹. Confirming the presence of the ν_{S-H} stretch in the spectrum of LB polymer film is more difficult than in the spectra of the 3C18-PMTT powder and their LB multilayers. It seems that this result indicates the progression of polymerization. However, the signal corresponding to the S-H stretching frequency is essentially weak in the case of IR. Hence, inductively coupled plasma mass spectrometry (ICP-MS) was performed on solutions of LB multilayers eluted from the solid. From the results of ICP-MS, it was found that this monolayer stoichiometrically contains Cd²⁺ on the -SH groups of poly[(3C18-PMTT)₂Cd]. This result is shown in Figure S2(a) in the Supporting Information. The sampling-procedure-eluted film molecules are drawn as in Figure S2(b). The

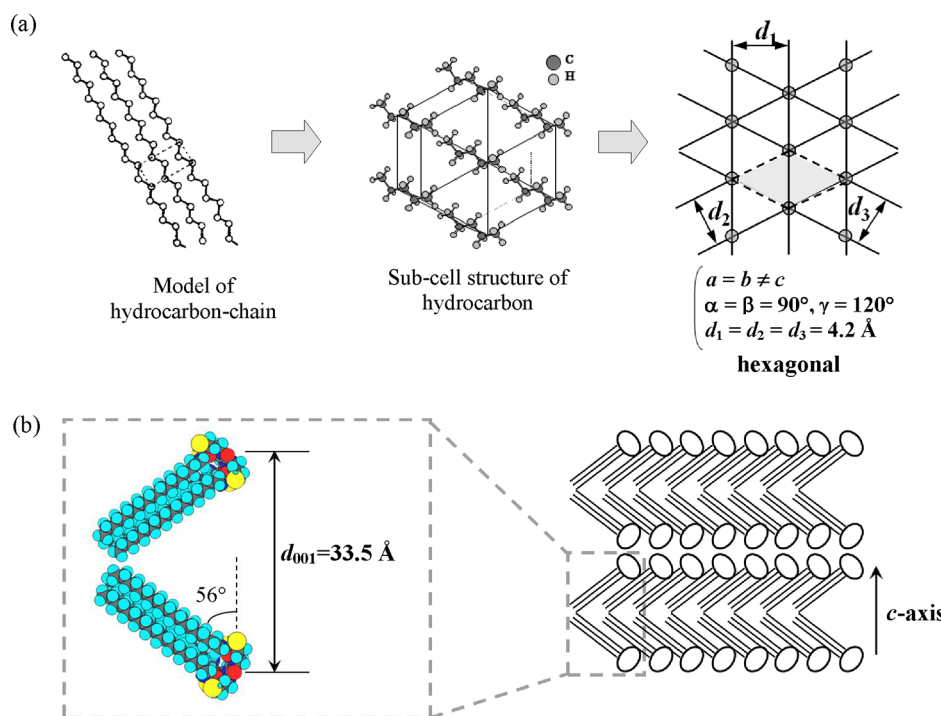


Figure 4. Chain packing and molecular arrangement models of 3C18-PMTT in the bulk.

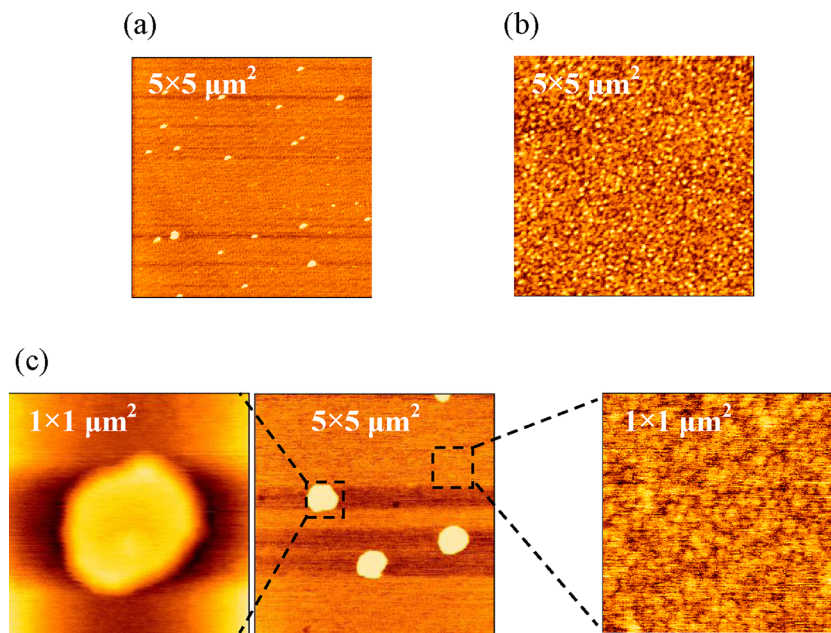


Figure 6. AFM images of Z-type monolayers of 3C18-PMTT at (a) 10, (b) 30, and (c) 45 mN m^{-1} on mica.

absolute value of Cd corresponds to $7.1 \mu\text{g}$. The ideal number of Cd atoms per monolayer unit is $1/2 \times 3 = 1.5/\text{unit}$. From the result of the calculation using the area per repeat unit of the isotherm, the amount of Cd in 20 layers on the solid surface corresponds to almost $7.16 \mu\text{g}$ (Figure S2(c)). This result indicates the stoichiometric complexing of Cd on the water surface. As a result, the effective progression of the chemical reaction of $n\text{R-SH} + \text{Cd}^{2+} \rightarrow n\text{R-S-Cd-S-nR} + n\text{H}^+$ exists at the air/water interface.

Figure 6 shows AFM images ($5 \times 5 \mu\text{m}^2$) of Z-type monolayers of the 3C18-PMTT monomer transferred onto a mica substrate at 10, 30, and 45 mN m^{-1} . For this system, on the mesoscopic scale there is not quite a smooth surface over all of the transferring surface-pressure region. In the low-surface-pressure region, dotlike domains appear. With an increase in surface pressure, a film-shaped structure gradually forms. Just before the collapse surface pressure, large domains of already piled up films are confirmed.

Figure 7 shows AFM images of Z-type poly[(3C18-PMTT)₂Cd] monolayers transferred onto a mica substrate at 5, 8, 20, and 30 mN m^{-1} . In this system, the morphological transition behavior is clear. At 5 mN m^{-1} , many circular nanodomains are constructed. These domains gradually coagulate with each other with increasing surface pressure, whereas domains in the corresponding monomer monolayer do not assemble. In the next step of the process, the coagulated domains aggregate to form a network structure with compression of the monolayer. Finally, a wide range of flat, homogeneous surfaces are formed in the monolayers of this metal-scavenged polymer. This monolayer indicates a relatively low defect surface in the higher-surface-pressure region. It is assumed that the poly[(3C18-PMTT)₂Cd] monolayer is an assembly of circular domains of different sizes. The polymer monolayer is quite stable to film compression, whereas the monomer is easily collapsed to a monomolecular film state. Relatively flat, homogeneous surface morphologies were obtained only by metal-scavenged polymerization at the air/water interface. It seems that stoichiometrical metal scavenging enhances the intermolecular interaction in the monolayers.

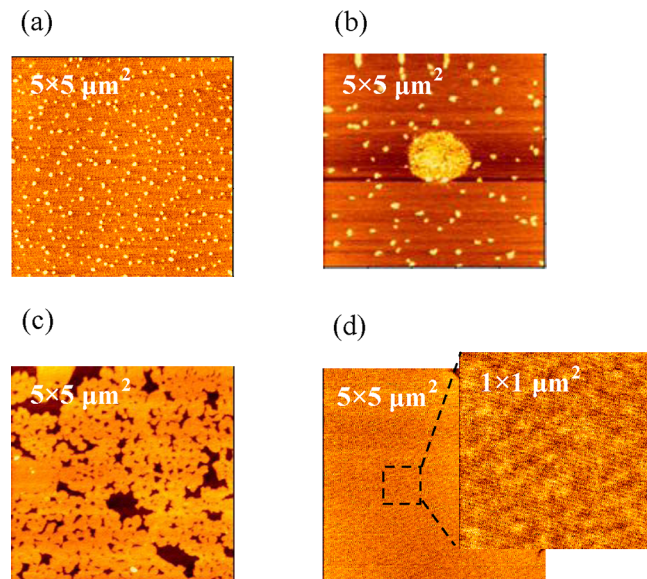


Figure 7. AFM images of Z-type monolayers of poly[(3C18-PMTT)₂Cd] at (a) 5, (b) 8, (c) 20, and (d) 30 mN m^{-1} on mica.

Molecular Arrangement of Organized Molecular Films of Poly[(3C18-PMTT)₂M]. To estimate the crystallinity and periodicity of the molecules in the monomer and corresponding polymer films, out-of-plane XRD and in-plane XRD of LB multilayers of the 3C18-PMTT monomer and poly[(3C18-PMTT)₂Cd] were performed. These systems were formed on distilled water and a buffer solution containing Cd²⁺ ions, respectively. These multilayers show a layer spacing of 52 Å along the *c* axis (Figure 8A). The organized molecular film shows developed layer structures with a larger spacing than that in the bulk state (Figure 2).

In-plane XRD measurements of these multilayers transferred by LB methods indicate that all 2D lattices of side chains form a hexagonal packing arrangement with a lattice spacing of 4.2 Å (Figure 8B). In the case of polymer multilayers, this (100) peak

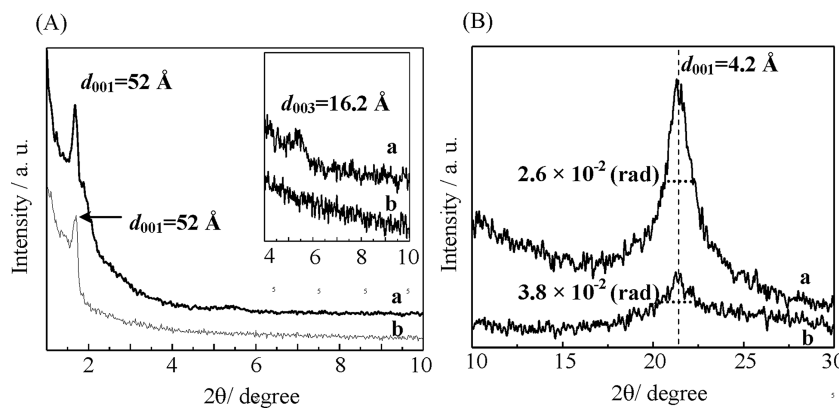


Figure 8. (A) Out-of-plane and (B) in-plane XRD profiles of multilayers (20 layers) of (a) poly[(3C18-PMTT)₂Cd] and (b) 3C18-PMTT. The crystallite size formed perpendicular to the (00l) plane is calculated by the Scherrer formula: (a) $D_{100} = 54.5 \text{ \AA}$ and (b) $D_{100} = 37.1 \text{ \AA}$.

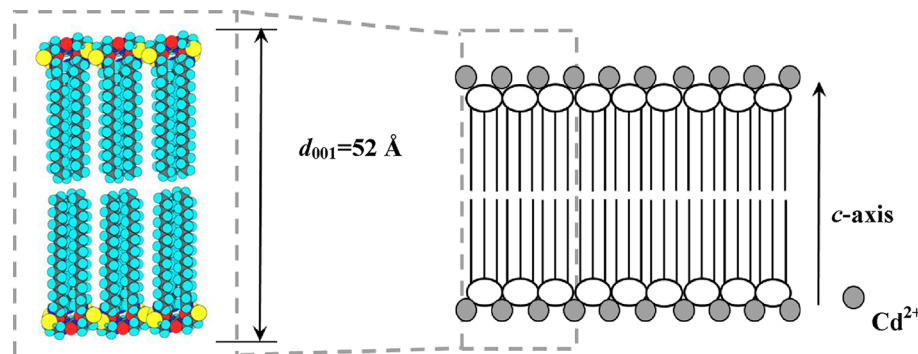


Figure 9. Schematic illustration of the molecular arrangement in layer structures of LB multilayers of poly[(3C18-PMTT)₂Cd].

of hexagonal packing is remarkably developed, which means that in the monolayer there is the formation of larger crystallite sizes than in the corresponding monomer. The crystallite size formed perpendicular to the (00l) plane is calculated by the Scherrer formula. Calculated crystallite sizes of polymer and monomer correspond to $D_{100} = 54.5 \text{ \AA}$ and $D_{100} = 37.1 \text{ \AA}$, respectively. The average diameters of crystallites in domains are enlarged by about 17 Å. That is to say, it is found that metal-scavenged polymerization enhances the crystallinity of the Langmuir monolayer.

To show the alignment along the *c* axis, a schematic illustration of 3C18-PMTT and the corresponding polymer is drawn in Figure 9. Both monomer and polymer films form a normal orientation of molecules. Although there is a slight difference between them, there is regularity in the layer structure of the polymer multilayers that is also developed in the monomer, as confirmed by a faint third-order reflection (inset of Figure 8A).

Figure S3 in the Supporting Information shows π -*A* isotherms of monolayers on a buffer solution containing Pd^{2+} ions for 3C18-PMTT and poly[(3C18-PMTT)₂Pd], corresponding AFM images of the transferred Z-type monolayer on mica, and the out-of-plane XRD spectrum of the LB multilayers. The inset of Figure S3(C) provides a schematic illustration of the molecular arrangement in the layer structure of the LB multilayers of poly[(3C18-PMTT)₂Pd]. Metal-scavenged polymerization progresses in the aqueous Pd solution. In this case, flexible beltlike domains are formed in the monolayer. These girdle domains aggregate to a uniform surface on the mesoscopic scale. A normal orientation with high regularity is also obtained in this case. Hence, it seems that this

type of metal-scavenged polymer monolayer forms homogeneous surfaces with high crystallinity and periodicity.

As mentioned previously, the amphiphilic compound with trithiol groups and three long hydrocarbons used in this study is polymerized at the air/aqueous metal solution interface as a polymer monolayer. This type of polymer monolayer indicates a rather flat surface with few defects. Furthermore, their multilayers are constructed as a highly ordered layer structure oriented perpendicular to the substrate. It is expected that this amphiphilic metal-scavenged polymer may be applied to the production of new nanoelectronic devices with a high periodicity of metals along the *c* axis and a homogeneous arrangement in the *ab* plane.

CONCLUSIONS

We investigated the solid-state structure, monolayer behavior on water and aqueous metal solution, mesoscopic morphological formation on a solid, and molecular arrangement of LB multilayers of an amphiphilic compound with metal-scavenging properties and their corresponding comb polymers. For this, we analyzed π -*A* isotherms, out-of-plane and in-plane XRD spectra, and AFM images. From the resultant AFM measurements, the formation of flat, homogeneous surface morphology of the polymer monolayer was confirmed. By estimation using the out-of-plane and in-plane XRD, the formation of highly ordered layer structures and hexagonal subcells is shown in organized films of this three-armed comb polymer. There is every possibility that these systems may bring about both the assurance of a supply of rare metal and rare earth elements and the production of new nanoelectronic materials.

Needless to say, the connection to the recovery of rare earth elements from oceans using LB films and in sufficient quantities to alleviate import restrictions is really a little too simplistic. The experimental results in this study do not exceed the scope of basic research. However, it is expected that this research will be a breakthrough for securing resources.

■ ASSOCIATED CONTENT

§ Supporting Information

IR spectra of 3C18-PMTT in the bulk, LB multilayers of 3C18-PMTT, LB multilayers of poly-[$(3\text{C}18\text{-PMTT})_2\text{Cd}$], and LB multilayers of poly-[$(3\text{C}18\text{-PMTT})_2\text{Pd}$]. Surface pressure-area isotherms of monolayers of poly[$(3\text{C}18\text{-PMTT})_2\text{Pd}$], corresponding AFM images of a Z-type monolayer on mica, and out-of-plane XRD of LB multilayers. Schematic illustration of the molecular arrangement in layer structures of LB multilayers of poly[$(3\text{C}18\text{-PMTT})_2\text{Pd}$].

This material is available free of charge via the Internet at <http://pubs.acs.org>.

■ AUTHOR INFORMATION

Corresponding Author

*E-mail: fujimori@fms.saitama-u.ac.jp. Tel and Fax: +81-48-858-3503.

Notes

The authors declare no competing financial interest.

■ ACKNOWLEDGMENTS

We greatly appreciate Dr. Atsushi Sasaki, Yamagata University, for his assistance with the ICP-MS measurements. We also thank Professor Keigo Matsuda, Yamagata University, for his assistance with the SEM observation and helpful discussions.

■ REFERENCES

- (1) Gaines, Jr., G. L. *Insoluble Monolayers at Liquid-Gas Interfaces*; Wiley: New York, 1966.
- (2) Kuhn, H.; Möbius, D.; Bücher, H. Spectroscopy of Monolayer Assemblies. In *Physical Methods of Chemistry*; Weissberger, A., Rossiter, B. W., Eds.; Wiley: New York, 1972; Vol. 1, Part IIIB, pp 577–702.
- (3) (a) Roberts, G. G. *Langmuir-Blodgett Films*; Plenum Press: London, 1990. (b) Petty, M. C. *Langmuir-Blodgett Films*; Cambridge University Press: New York, 1996.
- (4) Ulman, A. *An Introduction to Ultrathin Organic Films: From Langmuir-Blodgett to Self-Assembly*; Academic Press: Boston, 1991.
- (5) (a) Fukuda, K.; Shiozawa, T. Conditions for formation and structural characterization of X-type and Y-type multilayers of long-chain esters. *Thin Solid Films* **1980**, *68*, 55–66. (b) Fukuda, K.; Shiozawa, T. Structural control and characterization in mixed and alternate Langmuir-Blodgett films of simple long-chain compounds. *Thin Solid Films* **1989**, *178*, 421–425. (c) Fukuda, K.; Shibasaki, Y.; Nakahara, H. Effects of molecular arrangement on polymerization reactions in Langmuir-Blodgett films. *Thin Solid Films* **1983**, *99*, 87–94. (d) Fukuda, K.; Shibasaki, Y.; Nakahara, H. Molecular arrangement and polymerizability of amino acid derivatives and dienoic acid in Langmuir-Blodgett films. *Thin Solid Films* **1985**, *133*, 39–49. (e) Fukuda, K.; Shibasaki, Y.; Nakahara, H. Polymerizabilities of amphiphilic monomers with controlled arrangements in Langmuir-Blodgett films. *Thin Solid Films* **1988**, *160*, 43–52.
- (6) Spooner, S. P.; Whitten, D. G. Photoreactions in Monolayer Films and Langmuir-Blodgett Assemblies. In *Photochemistry in Organized & Constrained Media*; Ramamurthy, V., Ed.; VCH: New York, 1991; Chapter 15, pp 691–738.
- (7) *Probing of Proteins by Metal Ions and Their Low-Molecular-Weight Complexes*; Sigel, A., Sigel, H., Eds.; Marcel Dekker: New York, 2000; Vol. 38.
- (8) *Supramolecular Design for Biological Applications*; Obuhiko, Y., Ed.; CRC Press: Boca Raton, FL, 2002.
- (9) (a) Blodgett, K. Films Built by Depositing Successive Monomolecular Layers on a Solid Surface. *J. Am. Chem. Soc.* **1935**, *57*, 1007–1022. (b) Blodgett, K.; Langmuir, I. Built-Up Films of Barium Stearate and Their Optical Properties. *Phys. Rev.* **1937**, *51*, 964–982.
- (10) (a) Liu, M.; Kira, A.; Nakahara, H. Silver(I) Ion Induced Monolayer Formation of 2-Substituted Benzimidazoles at the Air/Water Interface. *Langmuir* **1997**, *13*, 4807–4809. (b) Gong, H.; Liu, M. In Situ Coordination of Coumarin 7 with Ag(I) at the Air/Water Interface: Characterization and Function of the Monolayers and Langmuir-Schaefer Films. *Langmuir* **2001**, *17*, 6228–6232. (c) Yuan, J.; Liu, M. Chiral Molecular Assemblies from a Novel Achiral Amphiphilic 2-(Heptadecyl) Naphtha[2,3]imidazole through Interfacial Coordination. *J. Am. Chem. Soc.* **2003**, *125*, 5051–5056.
- (11) Wang, K.; Haga, M.-A.; Hossain, M. D.; Shindo, H.; Hasebe, K.; Monjushiro, H. Effect of Subphase pH and Metal Ion on the Molecular Aggregates of Amphiphilic Ru Complexes Containing 2,2':6',2"-Terpyridine-4'-phosphonic Acid at the Air-Water Interface. *Langmuir* **2002**, *18*, 3528–3536.
- (12) Kmetko, J.; Datta, A.; Evmenenko, G.; Dutta, P. The Effects of Divalent Ions on Langmuir Monolayer and Subphase Structure: A Grazing-Incidence Diffraction and Bragg Rod Study. *J. Phys. Chem. B* **2001**, *105*, 10818–10825.
- (13) Kent, M. S.; Yim, H.; Sasaki, D. Y.; Majewski, J.; Smith, G. S.; Shin, K.; Satija, S.; Ocko, B. M. Segment Concentration Profile of Myoglobin Adsorbed to Metal Ion Chelating Lipid Monolayers at the Air-Water Interface by Neutron Reflection. *Langmuir* **2002**, *18*, 3754–3757.
- (14) Du, X.; Liang, Y. Roles of Metal Complex and Hydrogen Bond in Molecular Structures and Phase Behaviors of Metal *N*-Octadecanoyl-L-alaninate Langmuir-Blodgett Films. *J. Phys. Chem. B* **2000**, *104*, 10047–10052.
- (15) van Esch, J. H.; Nolte, R. J. M.; Ringsdorf, H.; Wildburg, G. Monolayers of Chiral Imidazole Amphiphiles: Domain Formation and Metal Complexation. *Langmuir* **1994**, *10*, 1955–1961.
- (16) Nagai, D.; Imazeki, T.; Morinaga, H.; Nakabatashi, H. Synthesis of a Rare-Metal Adsorbing Polymer by Three-Component Polyaddition of Diamines, Carbon Disulfide, and Diacrylates in an Aqueous/Organic Biphasic Medium. *J. Polym. Sci., Part A: Polym. Chem.* **2010**, *48*, 5968–5973.
- (17) Ochiai, B.; Ogiwara, T.; Mashiko, M.; Endo, T. Synthesis of Rare-metal Absorbing Polymer by Three-Component Polyaddition through Combination of Chemo-selective Nucleophilic and Radical Additions. *J. Am. Chem. Soc.* **2009**, *131*, 1636–1637.
- (18) Suzuki, A.; Nagai, D.; Ochiai, B.; Endo, T. Facile Synthesis and Crosslinking Reaction of Trifunctional Five-Membered Cyclic Carbonate and Dithiocarbonate. *J. Polym. Sci., Part A1* **2004**, *42*, 5983–5989.
- (19) Suzuki, A.; Nagai, D.; Ochiai, B.; Endo, T. Star-Shaped Polymer Synthesis by Anionic Polymerization of Propylene Sulfide Based on Trifunctional Initiator Derived from Trifunctional Five-Membered Cyclic Dithiocarbonate. *Macromolecules* **2004**, *37*, 8823–8824.
- (20) Jha, G. S.; Seshadri, G.; Mohan, A.; Khandal, R. K. Sulfur Containing Optical Plastics and Its Ophthalmic Lenses Applications. *e-Polym.* **2008**, *35*, 1–27.
- (21) Okutsu, R.; Suzuki, Y.; Ando, S.; Ueda, M. Poly(thioether sulfone) with High Refractive Index and High Abbe's Number. *Macromolecules* **2008**, *41*, 6165–6168.
- (22) Bearinger, J. P.; Terrettaz, S.; Michel, R.; Tirelli, N.; Vogel, H.; Textor, M.; Hubbell, J. A. Chemisorbed Poly(Propylene sulphide)-Based Copolymers Resist Biomolecular Interactions. *Nat. Mater.* **2003**, *2*, 259–264.
- (23) Kagaya, S.; Sato, E.; Masore, I.; Hasegawa, K.; Kanbara, T. Polythioamide as a Collector for Valuable Metals from Aqueous and Organic Solutions. *Chem. Lett.* **2003**, *32*, 622–623.

- (24) Chino, K.; Suga, K.; Ikawa, M.; Satoh, H. Novel Rapid-Cure Adhesives for Low Temperature Using Thiirane Compound. *J. Appl. Polym. Sci.* **2001**, *82*, 2953–2957.
- (25) Ogliari, F. A.; Sordi, M. L. T.; Ceschi, M. A.; Petzhold, C. L.; Demarco, F. F.; Piva, E. J. 2,3-Epithiopropyl Methacrylate as Functionalized Monomer in a Dental Adhesive. *Dentistry* **2006**, *34*, 472–477.
- (26) Ries, H. E. Films of Mixed Horizontally and Ly Oriented Compounds. *J. Colloid Sci.* **1961**, *16*, 361–374.
- (27) Fujimori, A.; Sugita, Y.; Nakahara, H.; Ito, E.; Hara, M.; Matsue, N.; Kanai, K.; Ouchi, Y.; Seki, K. Change of Molecular Packing and Orientation from Monolayer to Multilayers of Hydrogenated and Fluorinated Carboxylates Studied by in-Plane X-ray Diffraction Together with NEXAFS Spectroscopy at CK-Edge. *Chem. Phys. Lett.* **2004**, *387*, 345–348.
- (28) Fujimori, A.; Araki, T.; Nakahara, H.; Ito, E.; Hara, M.; Ishii, H.; Ouchi, Y.; Seki, K. In-Plane X-ray Diffraction and Polarized NEXAFS Spectroscopic Studies on the Organized Molecular Films of Fluorinated Amphiphiles with Vinyl Esters and Their Comb-Polymers. *Chem. Phys. Lett.* **2001**, *349*, 6–12.
- (29) (a) Shibaev, V. P.; Platé, N. A. Thermotropic Liquid-Crystalline Polymers with Mesogenic Side Groups. *Adv. Polym. Sci.* **1984**, *60/61*, 173–252. (b) Platé, N. A.; Shibaev, V. P. Comb-Like Polymers. Structure and Properties. *J. Polym. Sci., Macromol. Rev.* **1974**, *8*, 117–253.
- (30) (a) Inomata, K.; Sakamaki, Y.; Nose, T.; Sasaki, S. Solid-State Structure of Comb-Like Polymers Having n-Octadecyl Side Chains 0.1. Cocrystallization of Side Chain with n-Octadecanoic Acid. *Polym. J.* **1996**, *28*, 986–991. (b) Inomata, K.; Sakamaki, Y.; Nose, T.; Sasaki, S. Solid-State Structure of Comb-Like Polymers Having n-octadecyl Side Chains 0.2. Crystalline-Amorphous Layered Structure. *Polym. J.* **1996**, *28*, 992–999.
- (31) Fujimori, A.; Saitoh, H.; Shibasaki, Y. Influence of Molecular Arrangement on the Gamma-Ray-Irradiation Solid-State Polymerization of 1-Octadecyl Vinyl Ether with a Characteristic Polymorphism. *J. Polym. Sci., Part A1* **1999**, *37*, 3845–3853.
- (32) Fujimori, A.; Saitoh, H.; Shibasaki, Y. Polymorphism of Acrylic and Methacrylic Acid Esters Containing Long Fluorocarbon Chains and Their Polymerizability. *J. Therm. Anal.* **1999**, *57*, 631–642.